Dunai et al. p.1 DR; field photographs

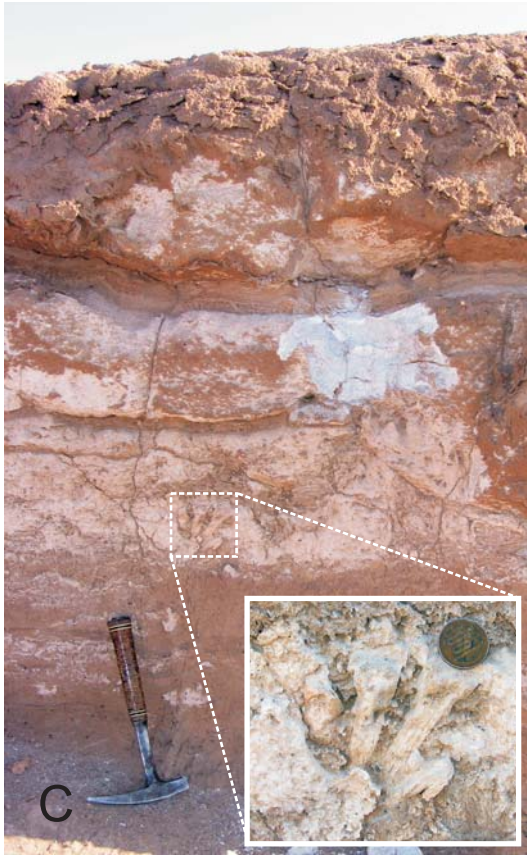

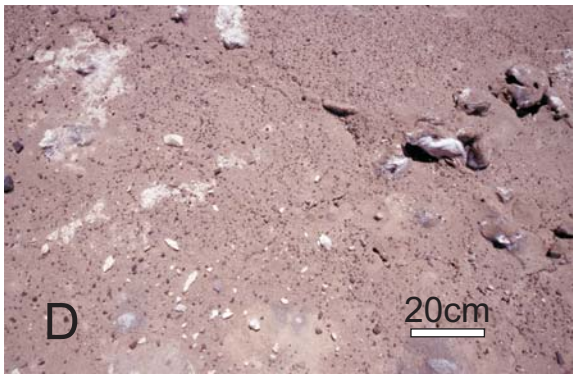

Figure caption DR1:

A) View to the west from site C. The thin, dark horizontal features at the base of the hills are the rims of the salt-karst pits around site B
B) Salt-karst pit at site B. Person in center as scale.
C) Evaporite profile showing intercalated salt (halite + anhydrite) and mud layers. Bottom nucleated gypsum crystals (inset), which are no anhydrite pseudomorphs, are indicative of an open water deposit (Warren, 1999). The evaporites in this area were deposited in a salina/mudflat setting (Tosdahl et al. 1984; Warren, 1999).
D) Quartz clasts (left center and foreground) at site B lying on salt (salt is mostly covered by a thin veneer of sand).
E) Gypsum crust with dispersed quartz clasts, as is typical for sites A & C. The quartz clasts sampled were 1 and 5 cm in size (minimum dimension).
F) Gravel pit at site D, coarse grain supported gravels with minor sand; partially carbonate cemented; paleo-groundwater level indicated by an undisturbed but friable carbonate-rich horizion at ~30 cm depth. Two arrows denote the sediment surface and the carbonate-rich horizon, respectively.

Tosdahl, R.M., Clark, A.H., and Ferrar, E., 1984 Cenozoic polyphase landscape and tectonic evolution of the Cordillera Occidental, southernmost Peru: Geological Society of American Bulletin. v. 95, p. 1318-1332.

Warren, J., 1999, Evaporites: Oxford, Blackwell, 438 p.

Table DR1; Isotope data, Dunai et al.

	type of sample	extraction	Elevation [m]	$^{21}Ne/^{20}Ne$	$^{22}Ne/^{20}Ne$	^{20}Ne [10^{10} atoms/g]	Excess ^{21}Ne [10^{8} atoms/g]	cosmogenic ^{21}Ne [10^{8} atoms/g]	Prod. Rate [atoms/g/a]	exposure age [Ma]
Site A										
PI03/1	amalg.	crush (150 x)	957	0.01049 ±0.00006	0.1145 ±0.0017	0.208 ±0.002	0.157 ±0.004			
		800º		0.19253 ±0.00087	0.328 ±0.0014	0.252 ±0.003	4.774 ±0.129	4.584 ±0.022	19.8	23.15 ±0.11
PI03/1	amalg.	crush (50 x)	957	0.00799 ±0.00008	0.1059 ±0.0064	0.139 ±0.002	0.07 ±0.003			
duplicate		crush (50 x)		0.01114 ±0.00009	0.1257 ±0.0192	0.063 ±0.001	0.051 ±0.002			
		crush (50 x)		0.01328 ±0.00015	0.0953 ±0.0351	0.03 ±0.000	0.031 ±0.001			
		400º		0.46155 ±0.00276	0.6367 ±0.0109	0.068 ±0.001	3.121 ±0.110	3.087 ±0.019		
		600º		0.14654 ±0.00087	0.2669 ±0.0069	0.107 ±0.001	1.535 ±0.054	1.481 ±0.009		
		800º		0.01333 ±0.00011	0.1096 ±0.0076	0.101 ±0.001	0.105 ±0.004	0.054 ±0.001		
							Total:	4.622 ±0.030	19.8	23.34 ±0.15
PI03/1 A	single clast	crush (150 x)	957	0.00493 ±0.00003	0.1039 ±0.0007	2.754 ±0.039	0.543 ±0.019			
		800º		0.0277 ±0.00016	0.1313 ±0.0008	2.174 ±0.030	5.379 ±0.188	4.95 ±0.036	19.8	25.00 ±0.18
PI03/1 B	single clast	crush (150 x)	957	0.00421 ±0.00002	0.1023 ±0.0004	4.819 ±0.067	0.6 ±0.021			
		800º		0.01765 ±0.00010	0.1189 ±0.0005	2.839 ±0.040	4.172 ±0.146	3.818 ±0.030	19.8	19.28 ±0.15
PI03/1 C	single clast	crush (150 x)	957	0.00482 ±0.00003	0.104 ±0.0007	2.132 ±0.030	0.397 ±0.014			
		800º		0.08121 ±0.00046	0.1942 ±0.0013	0.949 ±0.013	7.43 ±0.260	7.253 ±0.044	19.8	36.63 ±0.22
PI03/1 D	single clast	crush (150 x)	957	0.00488 ±0.00003	0.1049 ±0.0007	2.732 ±0.038	0.523 ±0.018			
		800º		0.03564 ±0.00022	0.1402 ±0.0011	1.505 ±0.021	4.919 ±0.174	4.631 ±0.033	19.8	23.38 ±0.17
Site B										
PI-06 A	single clast	crush (150 x)	925	0.00404 ±0.00003	0.1026 ±0.0006	3.002 ±0.042	0.323 ±0.011			
		800º		0.02559 ±0.00015	0.1272 ±0.0007	2.328 ±0.033	5.269 ±0.184	5.018 ±0.034	19.8	25.34 ±0.17
PI-06 B	single clast	crush (150 x)	925	0.00391 ±0.00002	0.1027 ±0.0005	2.967 ±0.042	0.282 ±0.010			
		800º		0.01774 ±0.00010	0.1191 ±0.0005	2.278 ±0.032	3.367 ±0.118	3.15 ±0.024	22	14.34 ±0.12
PI-06 C	single clast	crush (150 x)	925	0.00339 ±0.00002	0.1028 ±0.0006	2.177 ±0.030	0.093 ±0.003			
		800º		0.01787 ±0.00011	0.1196 ±0.0007	1.449 ±0.020	2.161 ±0.076	2.099 ±0.016	23.6	8.88 ±0.08
PI-06 D	single clast	crush (150 x)	925	0.00547 ±0.00003	0.1053 ±0.0007	0.119 ±0.002	0.03 ±0.001			
		800º		0.07429 ±0.00042	0.1867 ±0.0011	0.725 ±0.010	5.17 ±0.181	4.988 ±0.031	19.8	25.19 ±0.16

	type of sample	extraction	Elevation [m]	21Ne/20Ne	22Ne/20Ne	20Ne [10^{10} atoms/g]	Excess ^{21}Ne [10^{8} atoms/g]	cosmogenic ^{21}Ne [10^{8} atoms/g]	Prod. Rate [atoms/g/a]	exposure age [Ma]
Site C										
PI-07 A	single clast	crush (150 x)	931	0.00389 ±0.00003	0.1039 ±0.0009	1.401 ±0.020	0.13 ±0.005			
		800º		0.03712 ±0.00021	0.1432 ±0.0011	0.943 ±0.013	3.221 ±0.113	3.134 ±0.020	22	14.27 ±0.10
PI-07 B	single clast	crush (150 x)	931	0.00494 ±0.00003	0.1047 ±0.0007	1.874 ±0.026	0.37 ±0.013			
		800º		0.03508 ±0.00020	0.1401 ±0.0009	1.377 ±0.019	4.424 ±0.155	4.152 ±0.028	19.8	20.97 ±0.14
PI-07 C	single clast	crush (150 x)	931	0.00445 ±0.00003	0.1031 ±0.0005	3.146 ±0.044	0.47 ±0.016			
		800º		0.02879 ±0.00016	0.1319 ±0.0006	2.197 ±0.031	5.674 ±0.198	5.346 ±0.036	19.8	26.99 ±0.18
PI-07 D	single clast	crush (150 x)	931	0.00446 ±0.00003	0.103 ±0.0005	2.714 ±0.038	0.408 ±0.014			
		800º		0.01944 ±0.00011	0.1207 ±0.0005	2.646 ±0.037	4.361 ±0.152	3.963 ±0.030	19.8	20.01 ±0.15
Site D										
PI-11	amalg.	crush (150 x)	1023	0.00306 ±0.00002	0.1014 0.001	0.892 ±0.009	0.0087 ±0.0003			
	90 cm depth	800º		0.00312 ±0.00002	0.1003 0.0006	2.868 ±0.029	0.0464 ±0.0013	0.018 ±0.007		
PI-12	amalg.	crush (150 x)	1023	0.0031 ±0.00002	0.1011 0.0008	1.223 ±0.012	0.0168 ±0.0005			
	surface	800º		0.00318 ±0.00002	0.1021 0.0016	4.271 ±0.043	0.0927 ±0.0026	0.034 ±0.010	29.4	0.115 ±0.040
Site E										
PI-01	single clast	crush (150 x)	465	0.00309 ±0.00003	0.1061 0.0435	0.213 ±0.002	0.0027 ±0.0001			
		800º		0.00336 ±0.00002	0.1022 0.0011	0.87 ±0.009	0.0344 ±0.0010	0.023 ±0.004	19.2	0.122 ±0.022

Vein quartz clasts collected were 1–5 cm in size. The amalgamated samples from sites A and D as well as the sample from site E were crushed and sieved. From the 250-500 micron fraction we obtained the density fraction between 2.65 and 2.64 g/cm^3, which was subsequently chemically leached, first in dilute *aqua regia* at 60ºC, followed by three leaches in a dilute HF/NNO_3 mixture at 80ºC in an ultrasonic bath (Kohl and Nishiizumi, 1992). The density separation and the subsequent chemical leaching were aimed at removing quartz fragments with abundant fluid inclusions (Hetzel et al., 2002; Niedermann et al., 1994). The twelve individual clasts from sites A, B and C were crushed and cleaned in *aqua regia* at 60ºC. Due to the small sample size this material was not further leached. The 200-400 micron fraction was used for analysis.

Noble gas analysis of the quartz separates was carried out in the noble gas laboratory of the VU Amsterdam on a VG5400 mass spectrometer (Hanyu et al., 2001; van Soest et al., 1998). Gas extraction was accomplished by crushing in vacuum (Hanyu et al., 2001) and subsequent heating of the crushed sample in the crusher tube to 800ºC. On the amalgamated sample from site A we also performed a stepwise crushing and a stepwise heating (400, 600 and 800ºC) experiment. In the course of this work it turned out that a small fraction, 1-3 %, of the cosmogenic neon could be released by crushing. In order to determine the concentration of cosmogenic ^{21}Ne, the ^{21}Ne excess in the heated sample steps was calculated relative to the trapped component as revealed by crushing (Hetzel et al., 2002). Using this conservative approach, and neglecting the presence of the small amount of cosmogenic ^{21}Ne in the crushed sample steps, may lead to a small over-correction for trapped fluid inclusion hosted ^{21}Ne, i.e. the ages obtained can be up to 5% younger than they actually are.

U and Th concentrations were determined on five samples, including the amalmagated sample PI03/1. These concentrations were very low (<6 ppb in all cases), such that production of nucleogenic ^{21}Ne within the samples, which is produced by (alpha, n) reactions from ^{18}O and ^{19}F (Wetherill, 1954), can be excluded as a significant source of ^{21}Ne (assuming Cretaceous and Jurassic ages; i.e. the maximum ages of rocks in the potential source region). Further proof for the absence of any detectable nucleogenic component is the fact that the data for *all* data obtained plot within 1 sigma on the spallogenic line (i.e. the mixing line between pure atmospheric and pure cosmogenic Neon) in a ^{21}Ne/^{20}N vs. ^{22}Ne/^{20}Ne, three-isotope diagram (Niedermann et al., 1994). The slope of the regression line through the data is 1.1667 (R^2=0.998), which is indistinguishable from the expected value of 1.143±0.038 (Schäfer et al. 1997).

To calculate exposure ages from cosmogenic nuclide concentrations we use the production rate of ^{21}Ne (Niedermann, 2000) and the scaling procedures of (Dunai, 2000, 2001) taking the average Earth magnetic field strength over the last 800 kyr (Guyodo and Valet, 1999) as approximation for the long-term field intensity. Errors on the exposure ages do not include systematic uncertainties of the production rates, which are on the order of 10%. We use an average uplift rate of 40 m/Myr to calculate time-integrated ^{21}Ne production rates, since the sediments sampled at ~950 m were deposited near sea level.

To assess pre-exposure of average Azapa Formation sediments at sites A, B and C we use the samples from site D. At this site two samples were taken, one on the top of a well-preserved sediment bar in the riverbed, the other from a gravel pit (see also DR1 field photographs). Twenty-five vein quartz pebbles were collected for amalgamated samples at the surface of the bar and at 90 cm depth in the gravel pit in order to correct for an eventual inherited cosmogenic component. Porosity of the sandy gravel exposed in the pit is estimated at 30 ± 5%. The gravels in the riverbed contain the same lithologies as those exposed on the fault scarp east of site A (Figs. 2 and 3). The sediments in the riverbed were cannibalized from the valley flanks cut into sediments of the Azapa Formation.

Dunai, T.J., 2000, Scaling factors for production rates of in-situ produced cosmogenic nuclides: a critical reevaluation: Earth Planet. Sci. Lett., v. 176, p. 157-169.

—, 2001, Influence of secular variation of the geomagnetic field on production rates of in-situ produced cosmogenic nuclides: Earth Planetary Science Letters, v. 193, p. 203-218.

Guyodo, Y., and Valet, J.-P., 1999, Global changes in intensity of the Earth's magnetic field during the past 800 kyr: Nature, v. 399, p. 249-252.

Hanyu, T., Dunai, T.J., Davies, G.R., Kanoeka, I., Nohda, S., and Uto, K., 2001, Noble gas study of the Reunion hotspot: Evidence for distinct less-degassed mantle sources: Earth. Planet. Sci. Lett., v. 193, p. 83-98.

Hetzel, R., Niedermann, S., Ivy-Ochs, S., Kubik, P.W., Tao, M.X., and Gao, B., 2002, ^{21}Ne versus ^{10}Be and ^{26}Al exposure ages of fluvial terraces: the influence of crustal Ne in quartz: Earth Planet. Sci. Lett., v. 201, p. 575-591.

Kohl, C.P., and Nishiizumi, K., 1992, Chemical isolation of quartz for measurement of in-situ-produced cosmogenic nuclides: Geochim. Cosmochim. Acta, v. 56, p. 3583-3587.

Niedermann, S., 2000, The ^{21}Ne production rate in quarz revisited: Earth Planet. Sci. Lett., v. 183, p. 361-364.

Niedermann, S., Graf, T., Kim, J.S., Kohl, C.P., Marti, K., and Nishiizumi, K., 1994, Cosmic-ray-produced ^{21}Ne in terrestrial quartz: the neon inventory of Sierra Nevada quartz separartes: Earth Planet. Sci. Lett., v. 125, p. 341-355.

Schäfer, J.M., Ivy-Ochs, S., Wieler, R., Leya, I., Baur, H., Denton, G.H., and Schlüchter, C., 1999, Cosmogenic noble gas studies in the oldest landscape on Earth: Surface exposure ages of the Dry Valleys, Antarctica: Earth and Planetary Science Letters, v. 167, p. 215–226

van Soest, M.C., Hilton, D.R., and Kreulen, R., 1998, Tracing crustal and slab contributions to arc magmatism in the Lesser Antilles island arc using helium and carbon relationships in geothermal fluids: Geochim. Cosmochim. Acta, v. 62, p. 3323-3335.

Wetherill, G.W., 1954, Variations in the isotopic abundances of neon and argon extracted from radioactive minerals: Physical Review, v. 96, p. 679–683